

THE SINGLE-PARTICLE DENSITIES IN THE FISSION OF ^{258}Fm

M. WARDA

Institute of Physics, M. Curie-Skłodowska University
Pl. M. Curie-Skłodowskiej 1, 20-031 Lublin, Poland

(Received November 12, 2002)

Dedicated to Adam Sobiczewski in honour of his 70th birthday

The spontaneous fission of ^{258}Fm has been analysed in the constrained Hartree–Fock–Bogolubov calculations. The bimodal fission in this nucleus has been explained. The single particle energies and densities on the fission path have been investigated. The pre-scission formation of the fission fragments have been found.

PACS numbers: 21.10.Gv, 21.10.Pc, 21.60.Jz, 25.85.Ca

1. Introduction

The physics of the spontaneous fission of heavy nuclei has been quite well investigated over the last 50 years (see *e.g.* the review articles [1,2]). ^{258}Fm is a very specific nucleus in this area. The half-live time is smaller by seven orders of magnitude then its neighbour ^{256}Fm . The mass fragment distribution of ^{258}Fm is symmetric, with maximum at $A = 129$, whereas ^{256}Fm gives the asymmetric masses of fission products [3].

Furthermore, in contrast to the lighter nuclei, the fission of ^{258}Fm is the bimodal type [4,5]. In one mode the distribution of the total kinetic energy (TKE) of the two fragments has the maximum at 230 MeV, whereas in the other mode the mean TKE has the peak at 205 MeV. The two paths leading to the fission were found in the theoretical description of this process (*e.g.* [6–8]). In the first mode, referred to as the compact fission (CF) mode, the nucleus goes through shapes, consisting of two identical, touching spheres. The Coulomb repulsion in such a situation is relatively strong and causes the high TKE of the fragments.

The nucleus can also follow the path with reflection asymmetric shapes. In this case one part of the nucleus has a big deformation, whereas the other part remains almost spherical. The larger distance between the centres of

the mass of the two fragments at the scission point makes the Coulomb repulsion much weaker, and the mean TKE, smaller. This is referred to as the elongated fission (EF) mode.

In this paper, the analysis of the fission process of ^{258}Fm within self-consistent Hartree–Fock–Bogoliubov calculations with the Gogny forces has been done. In this constrained calculation, both the CF and the EF fission paths have been found. The difference in the TKE values and the mass distributions have been explained.

Apart from changes in the global properties of the nucleus during the fission, single particle (sp) properties have also been analysed. The sp energies and the densities of nucleons in each state have been determined. Those results are helpful in better understanding of the fission process. The two centres of the nuclear potential, created at the relative low deformation have been found. The pre-scission formation of the nuclear fragments has been proved.

In Sec. 2. the outline of the theory is presented. The results of our calculations are included in Sec. 3. Sec. 4. contains the conclusions of this paper.

2. Theory

The Gogny density-dependent effective nucleon–nucleon force was taken in the following form [9]

$$\begin{aligned}
 V_{12} = & \sum_{i=1}^2 (W_i + B_i \hat{P}_\sigma - H_i \hat{P}_\tau - M_i \hat{P}_\sigma \hat{P}_\tau) e^{-\frac{(\vec{r}_1 - \vec{r}_2)^2}{\mu_i^2}} \\
 & + i W_{\text{LS}} (\overleftarrow{\nabla}_1 - \overleftarrow{\nabla}_2) \times \delta(\vec{r}_1 - \vec{r}_2) (\overrightarrow{\nabla}_1 - \overrightarrow{\nabla}_2) \cdot (\vec{\sigma}_1 + \vec{\sigma}_2) \\
 & + t_0 (1 + x_0 \hat{P}_\sigma) \delta(\vec{r}_1 - \vec{r}_2) \left[\rho \left(\frac{\vec{r}_1 + \vec{r}_2}{2} \right) \right]^\gamma + V_{\text{Coul}}. \quad (1)
 \end{aligned}$$

The D1S [10, 11] parameterization of the Gogny interaction has been used. The microscopic self-consistent HFB equations have been solved [12] by expanding the quasiparticle creation and annihilation operators on finite bases of axially symmetric deformed harmonic oscillator eigenfunctions.

The basis used in calculations had one centre with $N_0 = 15$ oscillator shells in a direction perpendicular to the symmetry axis and $N_z = 22$ shells in z direction. This have made us possible describe more thoroughly very elongated shapes, which appear during the fission of the nucleus concerned.

In order to study different paths to fission in these calculations, the following constraints have been used: the axial quadrupole (Q_2), octupole (Q_3) and hexadecapole (Q_4) moments as well as the number of nucleons in the neck region (Q_N). The corresponding operators are given by

$$\hat{Q}_\lambda = r^\lambda P_\lambda(\cos(\theta)) \quad \text{and} \quad \hat{Q}_N = \exp\left(\frac{-z^2}{a_N^2}\right), \quad (2)$$

with $a_N = 1$ fm.

3. Results

3.1. Two fission modes

The shape of the potential energy surface provides the most important information on the spontaneous fission of nuclei. As it can be seen in Fig. 1, in ^{258}Fm the deformed ground state minimum is separated from the scis-

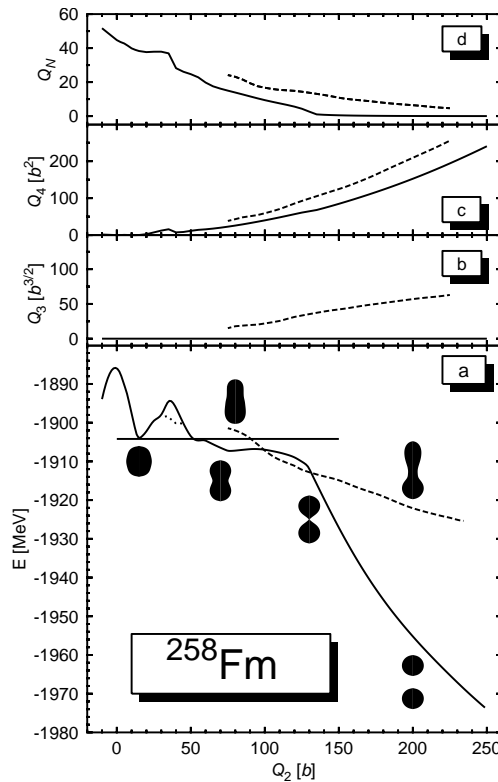


Fig. 1. (a): The fission barrier of ^{258}Fm as a function of the quadrupole moment Q_2 for $N_0 = 15$. The solid line corresponds to the compact fission path (CF) and the dashed line to the elongated one (EF). The dotted line shows the reduction of the first barrier due to nonaxial degrees of freedom. The shapes of the nucleus at a density of $\rho_0 = 0.08 \text{ fm}^{-3}$ are depicted for several values of Q_2 both for the CF and EF paths (note that the EF path leads to octupole deformed shapes). Additionally, in (b), (c) and (d) the octupole and hexadecapole moment as well as the neck parameter Q_N are plotted, respectively, [8].

sion point by the two-hump potential barrier [8]. The first hump is around 10 MeV high, but it can be decreased by a few MeV by including triaxial shapes in the calculations.

The two paths leading to the fission appear in the second minimum region. After tunneling the first barrier hump, the nucleus goes to the path on which the reflection symmetry is conserved. The shapes of the nucleus on this path consist of two touching spheres, which means that it produces the CF mode. The second path leads to asymmetric shapes ($Q_3 \neq 0$). The nucleus is built of one near spherical part and the deformed one. This path is responsible for the EF mode in the fission of ^{258}Fm .

The transfer to the asymmetric path is possible around $Q_2 = 90$ b, since the potential energy of the nucleus in both modes is similar in this region, and there is a small barrier separating them [8, 13].

3.2. Single-particle energies and densities

Beside the potential energy surface we can also determine the single-particle energies as a function of the quadrupole moment Q_2 . The results obtained for protons and neutrons along the CF path are presented in Fig. 2.

For small deformations with $Q_2 < 30$ b, the sp energy spectrum looks like the traditional Nilsson diagram. In the spherical nucleus, the main quantum number multiplets are well separated and the magic numbers can be easily obtained.

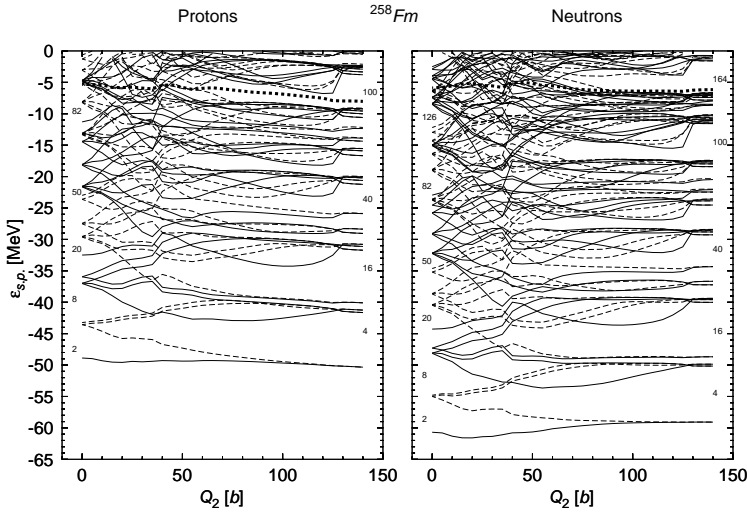


Fig. 2. The single-particle energies of ^{258}Fm nucleus in the CF mode for different Q_2 values. The positive parity states are plotted with the solid lines, while the negative parity states with the dashed lines.

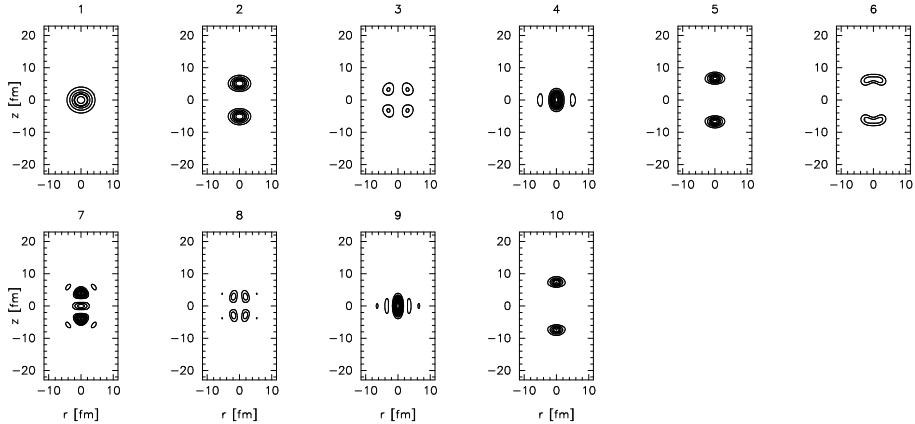


Fig. 3. The sp densities for $j = 1/2$ and positive parity in ^{258}Fm at $Q_2 = 15$ b. Labels describes the number of energy levels from the lowest one. The equidensity lines are plotted every 0.002 fm^{-3} as a function of r on the horizontal and z on the vertical axis.

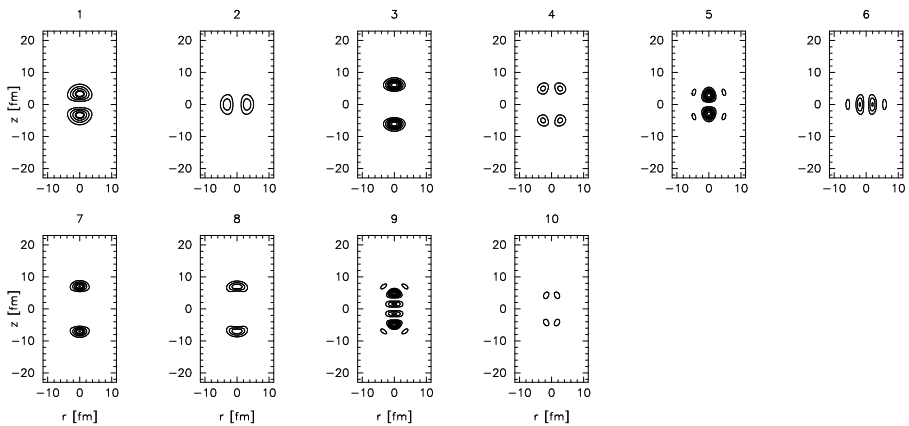


Fig. 4. The same as in Fig. 3, but for negative parity.

The new structure appears from the chaotic level spectrum at $Q_2 \sim 50$ b. The lowest levels (with $E < 35$ MeV) are grouped into blocks. Going to the higher deformations, more groups can be found. The energy gaps separating them correspond to doubled magic numbers (*i.e.* 4, 16, 40, 56, 100 and 164).

In each group, the pairs of the states with positive and negative parity and the same total angular momentum are coupled. Finally four-times degenerated levels are created. The nucleons which these levels are comprised of differ only in parity and spin quantum numbers. At the scission point, multiplets, characteristic for spherical nuclei, are created again.

These results can be easily explained if compared with the shape of nucleus at the scission point. The nucleus is built from two spherical parts. From each of them, a new, spherical, daughter nucleus ^{129}Sn is created. The sp energies must change their arrangement to the ones corresponding to the fission products. In fact, the two-centre system, manifesting the creation into two Sn nuclei, appears much before scission point.

The similar conclusion can be derived from the analysis of sp densities. In the ground state, at $Q_2 = 15$ b sp densities correspond to the orbitals of an electron in a hydrogen atom. As an example, the densities of protons with $j = 1/2$ and positive and negative parities are presented in Figs. 3 and 4, respectively.

The sp wave function and densities evolve with an increase in deformation. At low quadrupole moments, sp densities deform their shapes, preserving ground state scheme. At the larger deformations, the two-centre structure is created. The rearrangement of the two lowest $j = 1/2$ proton energy states of both parities at the CF path is shown in the Fig. 5. For these particles splitting into two centres can be noticed already at $Q_2 = 40$ b. At $Q_2 = 80$ b the density at the central point of the nucleus decreases to zero. Moreover, from $Q_2 = 100$ b the sp densities are identical in the case of the two lowest energy levels. The nucleons in these states are well located in the new created centres.

The same scenario is repeated for the other pairs of levels with the same j and opposite parities. The general tendency is that states with higher energy start to transform their orbitals at higher deformations.

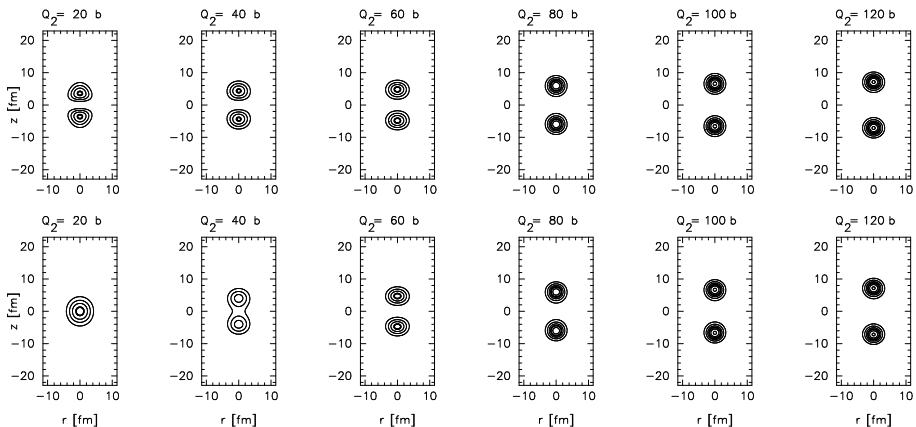


Fig. 5. The sp densities for the lowest (lower row) and the second lowest (upper row) $j = 1/2$ energy states in ^{258}Fm for different Q_2 values. The equidensity lines are plotted every 0.002 fm^{-3} as a function of r on the horizontal and z on the vertical axis.

In Figs. 6 and 7, proton states with $j = 1/2$ are presented again, yet at the deformation very close to the scission point with $Q_2 = 120$ b. In Fig. 6 states with positive parity and in Fig. 7 with negative parity are shown. The first three density distributions are identical in both figures. In the following panels the two centre structure can also be found, but the formation of the fission fragments is not complete yet. The maximum of the sp density at $z = 0$ can be even found for some states.

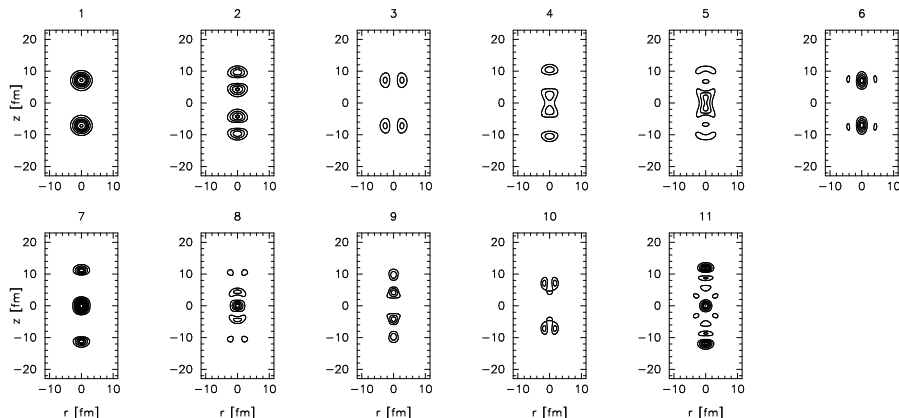


Fig. 6. The same as in Fig. 3, but at $Q_2 = 120$ b.

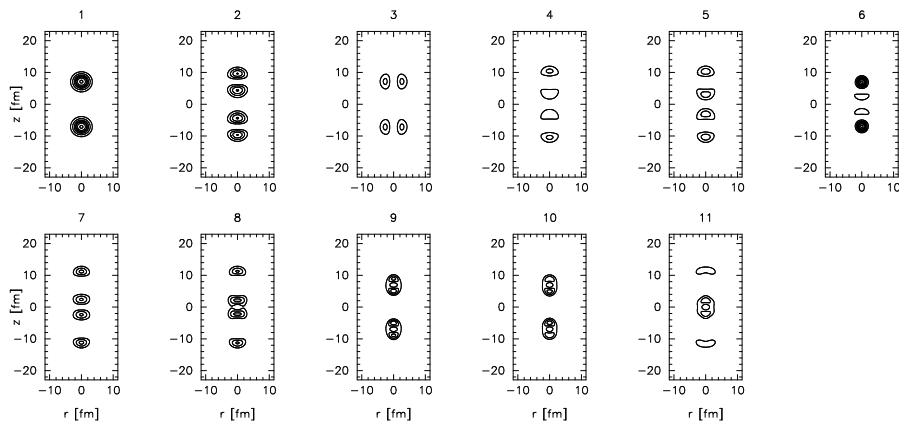


Fig. 7. The same as in Fig. 7, but for negative parity.

These results are consistent with the results of the two-centre shell model [14]. Although we deal with one centre deformed basis, the cluster structure with two centres is obtained by selfconsistent calculations.

The situation is slightly different in the case of EF mode. The reflection symmetry between the two parts is broken and energy levels in this mode can not couple into pairs (see Fig. 8). There are no such well defined energy gaps as in the CF mode. The sp energies do not vary significantly (espe-

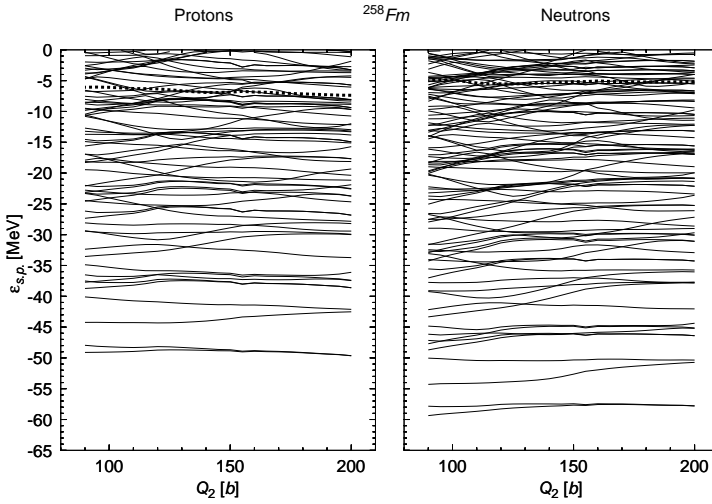


Fig. 8. The single-particle energies of ^{258}Fm nucleus in the EF mode for different Q_2 values.

cially in the low energy states) even if big changes in the deformation of the nucleus are concerned. In the EF mode, changes in quadrupole moment are connected with an increase in the distance between the centres of the fragments. This does not affect strongly the nucleons in the states that are located in one of the clusters.

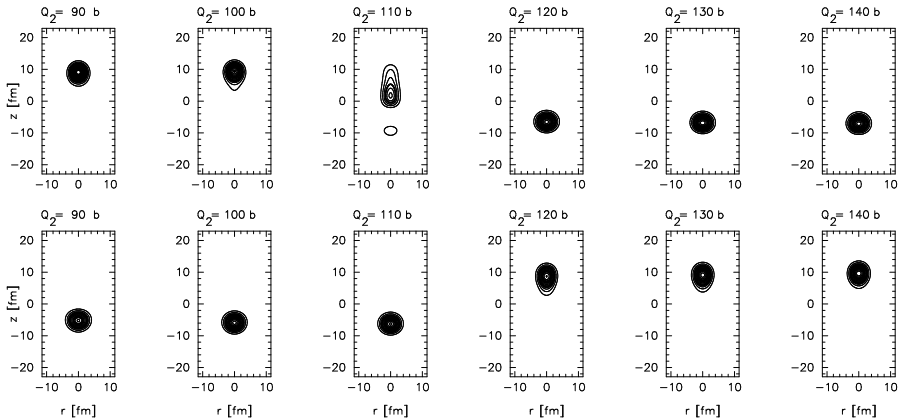


Fig. 9. The single-particle energies of ^{258}Fm nucleus in the EF mode for different Q_2 values.

The nucleons in some low energy quantum states are shifted completely to the one of the nuclear parts (see Fig. 9, where two the lowest energy states are in the centres of two creating fragments of the nucleus). However, some sp densities are spread out through entire the nucleus for all deformations, and do not take part in pre-scission nucleus formation (Fig. 10).

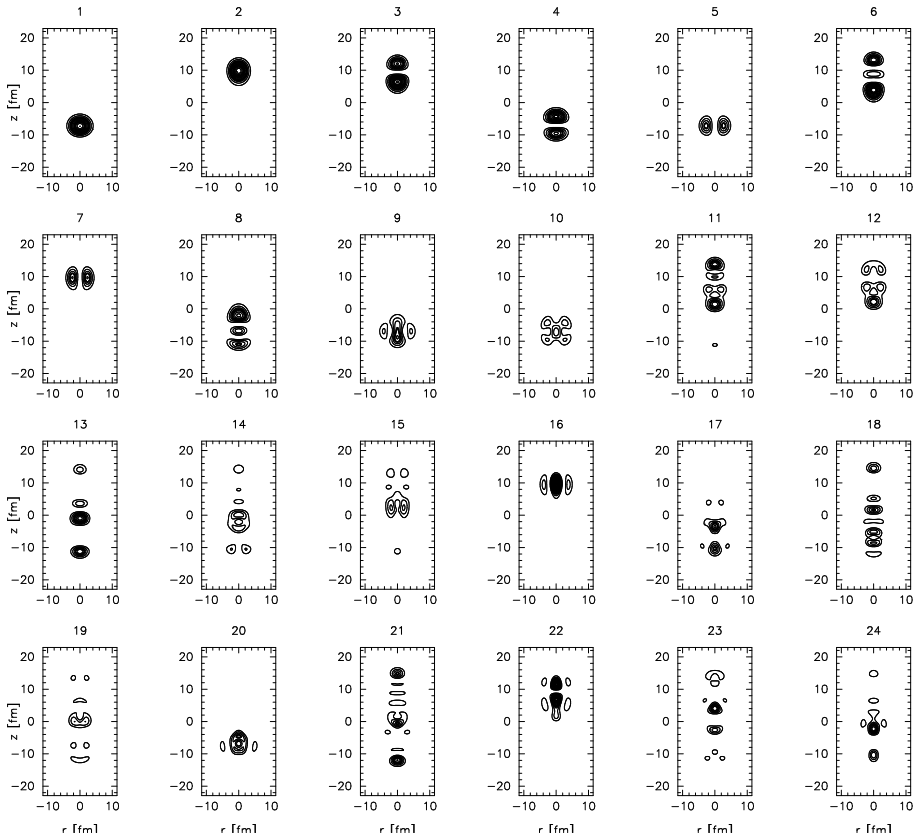


Fig. 10. The sp densities for $j = 1/2$ in ^{258}Fm at $Q_2 = 150$ b in the EF mode. Descriptions are the same as in Fig. 3.

4. Conclusions

Two fission paths were found in ^{258}Fm : the symmetric one leading to the compact fission and the reflection asymmetric corresponding to the elongated fission in the total kinetic energy distribution. The splitting of the nucleus into two fragments begins before the scission point. The nucleons from the deepest energy levels separate their orbitals already in the second minimum ($Q_2 = 50$ b). In the compact mode four-times degenerated energy levels are

created with two pairs of nucleons in each centre of the system. The energy structure of fragments to be created in the fission is manifested before the scission point.

In the EF mode no groups in the energy spectrum can be noticed. The nucleons with low energy are located in the spherical or in the deformed part of the nucleus.

The agreement of these results with the two-centre shell model proves that the deformed basis chosen in our calculations is sufficient for the description of the nuclear fission.

This work is partly sponsored by the Polish State Committee for Scientific Research, grant No. 2P 03B 115 19. The author would like to thank K. Pomorski for fruitful collaboration, and J.L. Egido, L.M. Robledo for helpful discussions and the fortran code used in calculations.

REFERENCES

- [1] D.C. Hoffman, *Nucl. Phys.* **A502**, 21c (1989).
- [2] F. Gönnerwein, *Nucl. Phys.* **A654**, 855c (1999).
- [3] R. Vandenbosch, J.R. Huizenga, *Nuclear Fission*, Academic Press, New York 1973.
- [4] E.K. Hulet, J.F. Wild, R.J. Dougan, R.W. Loughheed, J.H. Landrum, A.D. Dougan, M. Schädel, R.L. Hahn, P.A. Baisden, C.M. Henderson, R.J. Dupzyk, K. Sümmerer, G.R. Bethune, *Phys. Rev. Lett.* **56**, 313 (1986).
- [5] E.K. Hulet, J.F. Wild, R.J. Dougan, R.W. Loughheed, J.H. Landrum, A.D. Dougan, P.A. Baisden, C.M. Henderson, R.J. Dupzyk, M. Schädel, K. Sümmerer, G.R. Bethune, *Phys. Rev.* **C40**, 770 (1989).
- [6] S. Ówiok, P. Rozmej, A. Sobiczewski, Z. Patyk, *Nucl. Phys.* **A491**, 281 (1989).
- [7] P. Möller, J.R. Nix, *Nucl. Phys.* **A549**, 84 (1992).
- [8] M. Warda, J.L. Egido, L.M. Robledo, K. Pomorski, *Phys. Rev.* **C66**, 014310 (2002).
- [9] J. Dechargé, D. Gogny, *Phys. Rev.* **C21**, 1568 (1980).
- [10] J.F. Berger, M. Girod, D. Gogny, *Nucl. Phys.* **A428**, 23c (1984).
- [11] J.F. Berger, M. Girod, D. Gogny, *Comput. Phys. Commun.* **63**, 365 (1991).
- [12] J.L. Egido, L.M. Robledo, R.R. Chasman, *Phys. Lett.* **B393**, 13 (1997).
- [13] M. Warda, J.L. Egido, L.M. Robledo, K. Pomorski, to be published in *Phys. At. Nucl.*
- [14] D. Scharnweber, W. Greiner, U. Mosel, *Nucl. Phys.* **A164**, 257 (1971).